Progress In Electromagnetics Research C, Vol. 120, 243–252, 2022

Design of a Wideband ME Dipole Antenna with Wide Beamwidth

Haoyu Fang[1], Jianfeng Sun[1], Hao Zhang[1], Yiqing Liu[2], and Zhuopeng Wang[1, *]

Abstract—A wideband and widebeam magneto-electric (ME) dipole antenna is designed in this paper. Based on the conventional magneto-electric dipole antenna, a bent vertical metal plate is added to the electric dipole, and the impedance bandwidth (IBW) and beamwidth of the antenna are widened together. Inclined metal walls are added on both sides of the metal ground to improve the gain at high frequency and make the antenna gain more steady in the operating bandwidth. To further broaden the IBW of the antenna, the conventional Γ-shaped feed is changed into a branch structure. The IBW of the finally designed antenna reaches 56.8% (2.91–5.22 GHz). In the whole operational bandwidth, the radiation pattern in E-plane realizes the half power beamwidth (HPBW) of more than 110°, and the H-plane radiation pattern realizes the HPBW of more than 160°. The maximum width of E-plane HPBW is 175°, and the maximum width of H-plane HPBW is 229°.

1. INTRODUCTION

In wireless communication systems in open areas such as suburbs, antennas are expected to have wide beam characteristics to extend the coverage of signals and need to have wide band characteristics to increase the information capacity. In recent years, scholars have tried various methods to broaden the beam of antennas. In [1], a wide-beam planar patch antenna was proposed with a reflective structure attached to one side of the antenna patch to widen the beam, reaching a beamwidth about 140° in E-plane and less than 55° in H-plane in the −10 dB impedance bandwidth (IBW) from 0.9 to 2.6 GHz. In [2], a hybrid zero-order resonant patch antenna with a wide planar beamwidth is designed. By inserting the mushroom antenna into a rectangular patch antenna with an etched rectangular hole, both the TM_{010} mode and ZOR mode are created, thus spreading the beamwidth of the antenna. The presented antenna achieves a beamwidth of 115° in the E-plane, which is 53% higher than that of a conventional microstrip antenna. In [3], a triple current model is presented to design a wide-beam onboard antenna. The three currents can excite the equal amplitude in the five directions of the hemispherical pattern to realize wide-beam radiation. A wide-beam vehicle antenna is designed based on this model. With the edge length of the bottom plane being 2λ, the half power beamwidth (HPBW) in E-plane and H-plane can reach 141° and 148°. In [4], the radiation beam of a patch antenna is widened by using a circular patch and independently fed concentric metal rings, and the HPBWs in E-plane and H-plane reach 258° and 267°, respectively. Although the antennas designed in [2–4] all achieve wide-beam characteristics, the operating bandwidths of the antennas are relatively narrow.

Magneto-electric (ME) dipole antenna was first presented by Luk and Wong [5], which is a complementary antenna that combines current and equivalent magnetic current with the advantages of stable radiation pattern and low cross-polarization. A variety of wide-beam ME dipole antennas have been presented by researchers. In [6], a wide H-plane beamwidth ME dipole antenna was designed, and the H-plane beamwidth was spread to 120° by folding the ground plane into a trapezoidal shape and by

Received 16 March 2022, Accepted 25 May 2022, Scheduled 11 June 2022

* Corresponding author: Zhuopeng Wang (wzhuopeng1@sdust.edu.cn).

[1] College of Electronic and Information Engineering, Shandong University of Science and Technology, China. [2] College of Electrical Engineering and Automation, Shandong University of Science and Technology, China.

adding slots in the electric dipole. In [7], by using a slanted electric dipole and changing the structure of the electric dipole and ground, a beamwidth about 100° was achieved in both the E-plane and H-plane in the 1.9–2.7 GHz band. A planar ME dipole antenna was designed in [8], and the three short edges of a rectangular patch are considered as magnetic dipoles and the open edge as electric dipole. By introducing the magnetic dipole into the planar dipole antenna, an E-plane beamwidth of 140° is achieved, but the −10 dB IBW of the antenna is only 4.1% (5.73 GHz–5.96 GHz). A magnetoelectric dipole antenna proposed in [9] achieves multiband wide-beam characteristics through four Γ-shaped metal plates, but with a relatively narrow beamwidth in the high frequency band.

Although a large number of achievements have been made in the research of wide-beam antenna [10–16], there are few reports on the antenna that can meet the broadband operation and realize the wide-beam characteristics in both E-plane and H-plane. Based on the conventional ME dipole, a wideband and wide-beam ME dipole antenna is presented in this paper. By appropriately improving the structure of metal plates, ground plane, and feed line, the beamwidth and operating bandwidth of the antenna are broadened, and the HPBW of more than 110° can be realized in the wide operational frequency band in both E plane and H plane. The designed antenna has stable gain and low cross polarization in the operating bandwidth.

2. ANTENNA DESIGN

2.1. Antenna Geometry

The geometric structure of the designed antenna is shown in Figure 1. The antenna consists of a metallic ground, a branched and deformed Γ-shaped feed line, and a pair of metal plates as electric and magnetic dipoles. The feed line excites the vertical metal surfaces on both sides to form a magnetic dipole, and two horizontal metal sheets act as electric dipoles. Compared with the initial magneto-electric dipole in [5], the Γ-shaped feed line is branched to both sides to widen the impedance bandwidth of the antenna. A bent metal plate is loaded on the electric dipole to spread both the bandwidth and beamwidth of the antenna. The two sides of the ground are bent upward to form two inclined metal walls to improve the antenna gain. The overall size of the antenna is $31 * 22 * 15$ mm. The geometric parameters of the presented antenna are shown in Table 1.

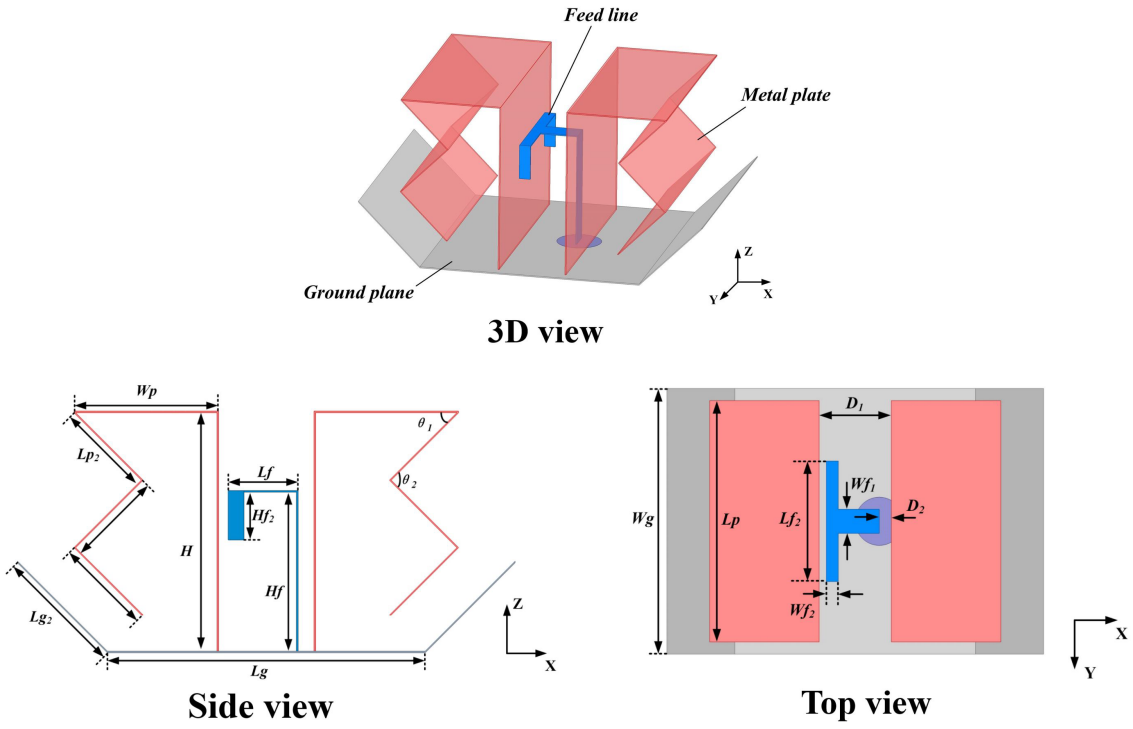

Figure 1. Antenna configuration.

Table 1. Dimension parameters of the presented antenna (Unit: mm).

Parameter	Value	Parameter	Value	Parameter	Value
Lg	20	**Wp**	9	**Wf_1**	2
Lg_2	8	**Hf_2**	3	**Wf_2**	1
Wg	22	**D_2**	0.9	**H**	15
Lp	20	**Lf**	4.4	**Hf**	10
Lp_2	6	**Lf_2**	10	**D_1**	5.8

2.2. Antenna Mechanism

The design process of the antenna is depicted in Figure 2. The reflection coefficients (S_{11}) of the antennas with different structures are shown in Figure 3(a). Ant.1 is a conventional ME dipole antenna structure, which has a narrow impedance bandwidth and does not have wide beam characteristics. In order to improve the antenna performance, the radiation structure of the antenna is considered to be modified. Ant.2 adds vertical metal plates to the electric dipoles compared with Ant.1, so that the radiation pattern of antenna can be generated by both horizontal and vertical currents, thus widening the antenna beamwidth. The change of the antenna current distribution also improves the impedance matching of the antenna, and the impedance bandwidth of the antenna is broadened. The addition of vertical metal plates makes the operating band of Ant.2 shifted to high frequency compared with Ant.1, and the gain curve has also shifted simultaneously. To extend the current path in the vertical direction, Ant.3 bends the vertical metal plates compared to Ant.2 (bending angle: $\theta_1 = 45°$, $\theta_2 = 90°$), which further widens the beamwidth. The radiation patterns of each antenna model at 4.7 GHz are shown in Figure 4.

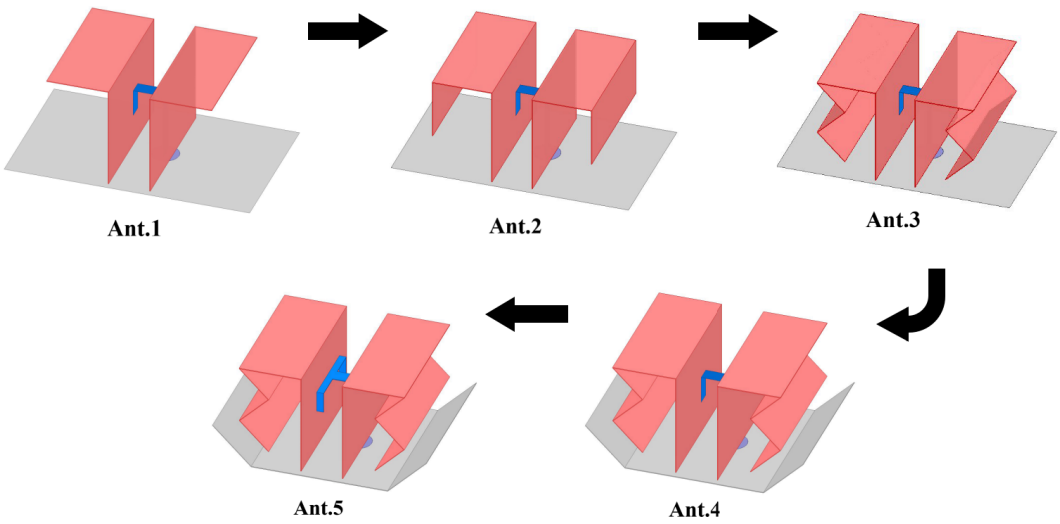

Figure 2. Design evolution of proposed antenna.

However, the antenna gain is not stable in the operating bandwidth and decreases sharply at high frequencies. To solve this problem, both sides of the metal ground are bent upward 45° to form two inclined metal walls, that is, the structure of Ant.4 is shaped. Due to the coupling effect of the metal wall and the bent metal plate connected to the electric dipole on the antenna radiation, the antenna gain at high frequency rises, and the antenna obtains a steady gain in the whole operational bandwidth, as shown in Figure 3(b). Since Ant.4 has higher gain than Ant.3, the beamwidth is relatively narrow, but still wider than the beamwidth of Ant.2. Finally, to further widen the impedance bandwidth, the

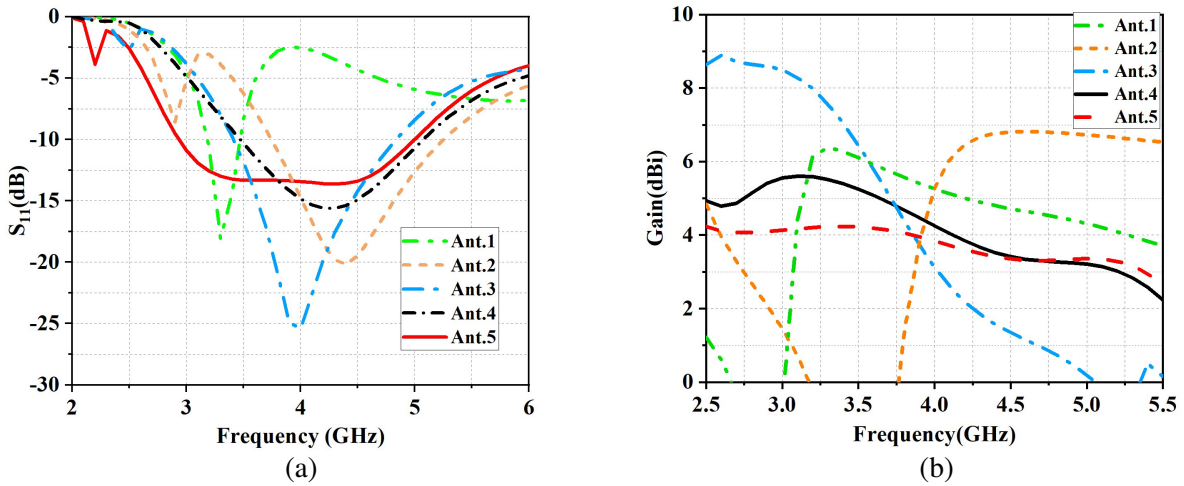

Figure 3. (a) Simulated S_{11} and (b) gain of Ant.1–5.

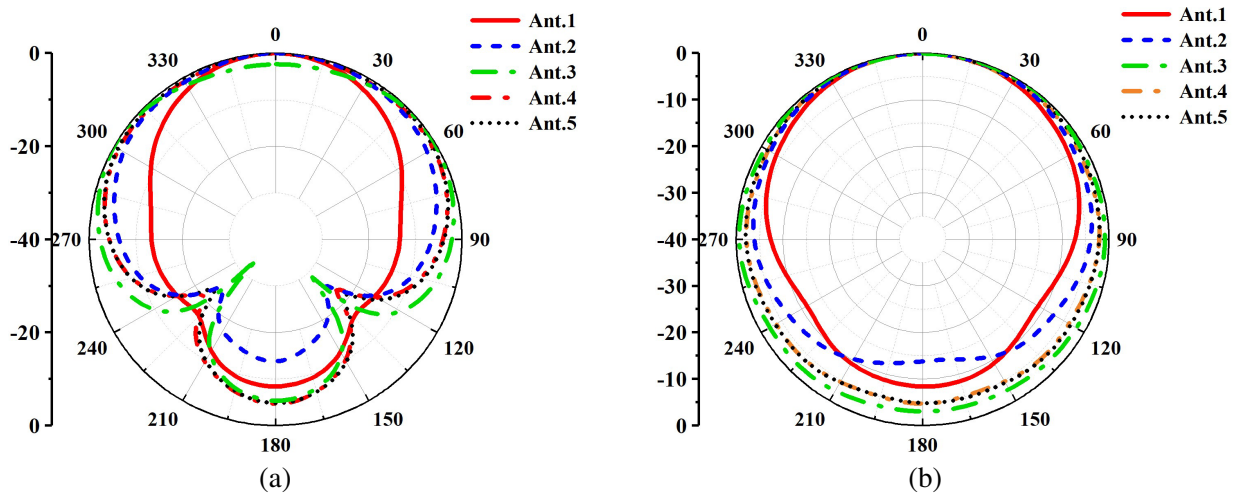

Figure 4. Simulated radiation patterns of Ant.1–5. (a) E-plane, (b) H-plane.

feed line of the antenna is modified, and the original Γ-shaped feed line is branched to both sides, so that the −10 dB IBW of the antenna is increased from 37.7% (3.47–5.08 GHz) to 51.9% (2.94–5.0 GHz). The principle of bandwidth spreading can be explained by analyzing the input impedance of the antenna. As shown in Figure 5, the input impedance of Ant.4 presents capacitive at low frequency (< 4 GHz), which makes the impedance matching of the antenna at low frequency band poor. Ant.5 modifies the feed line of Ant.4 into a branch structure to increase the inductance of the feed line, which compensates for the capacitive nature of the feed structure at low frequencies and improves the impedance matching of the antenna at low frequency band, thus effectively expanding the operating bandwidth of the antenna.

Figure 6 depicts the surface current distribution of the presented antenna at center frequency 4 GHz. As the phase is 0°, the surface current on the horizontal metal plate points to the same direction; the current on the two vertical metal plates near the feed line is relatively weak; and the electric dipole plays the main role. The current in the vertical direction is generated on the bent metal plate, and the direction is opposite, which supplements the weak region in the main radiation direction. At the 90° phase, the surface current on the horizontal metal sheet is weak; the current on the vertical metal plate is strong; and the magnetic dipole plays a main role. At the 180° phase, the current direction is opposite to that when the phase is 0°; the surface current is concentrated in the horizontal metal

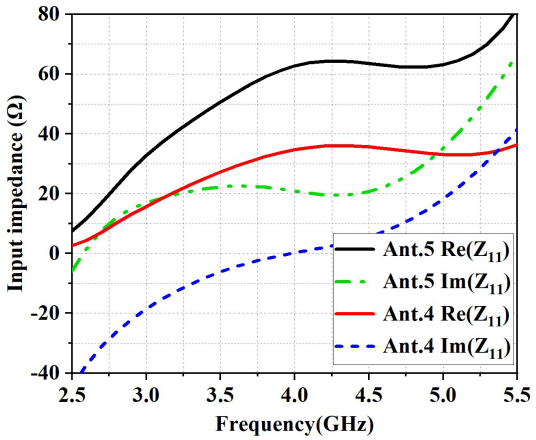

Figure 5. Simulated input impedance of Ant.4 and Ant.5.

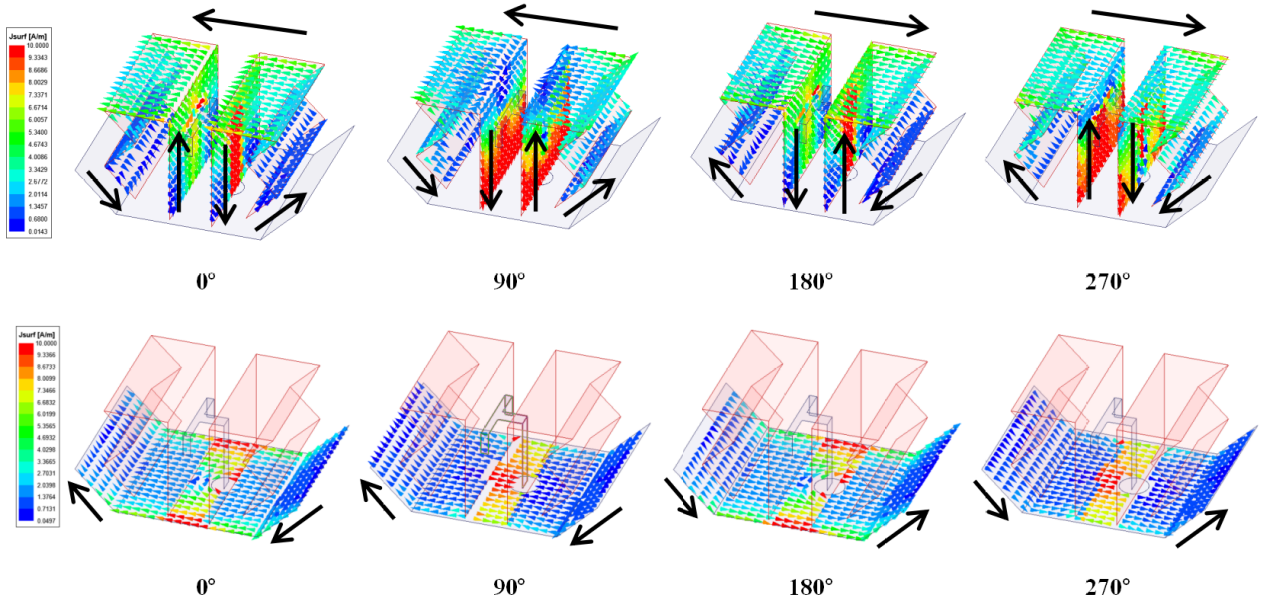

Figure 6. Simulated surface current distributions at 4 GHz.

plate; and the antenna radiation is mainly generated by the electric dipole. When the phase is 270°, the current direction is opposite to that when the phase is 90°, and the antenna radiation is mainly generated by magnetic dipole. According to the above analysis, changing the structural size to adjust the amplitude and phase of the electric dipole and magnetic dipole can make the antenna work in a wide bandwidth and achieve stable radiation. The current direction of the antenna ground also changes periodically. The sidewalls of the ground and the bent metal plates connecting the electric dipoles form a capacitive coupling, obtaining a loop-like current distribution between them, thus the gain of the antenna is improved.

Figure 7 shows the electric field intensity distribution in the XOZ and YOZ planes at 4 GHz. The analysis of the electric field distribution can further explain the principle of the antenna to achieve wide beam radiation. In XOZ plane, due to the radiation of electric dipole, the electric field distribution in the area above the antenna is more concentrated. At the same time, due to the combined effect of the bent metal plate connected to the electric dipole and the inclined metal wall connected to the ground, a concentrated area of electric field is produced on the left and right sides, which proves that

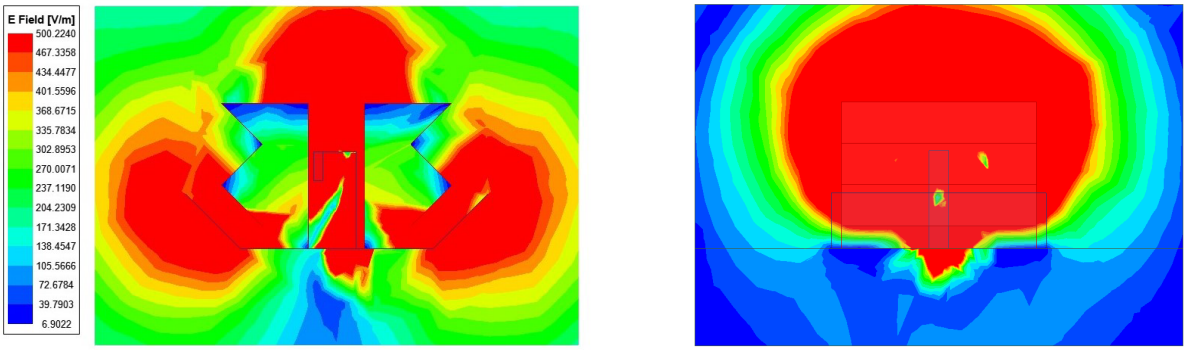

Figure 7. Simulated electric field distributions at 4 GHz. (a) XOZ-plane, (b) YOZ-plane.

the bent metal plate and inclined metal wall supplement the radiation on both sides of the antenna. In the YOZ plane, the electric field is mainly concentrated above the antenna, and because the antenna has a narrow ground, a strong electric field is also generated on the two sides of antenna, indicating that the antenna also has a wide beamwidth in this plane.

2.3. Parametric Study

The antenna is simulated and analyzed to investigate the effect of the structural dimensions of the antenna on the antenna performance. Here, the spacing of electric dipoles D_1, the antenna's feedline width Wf_1, and the length of the inclined metal wall Lg_2 are analyzed.

Figure 8 shows the variations of antenna reflection coefficient and HPBW with electric dipole spacing D_1. It can be observed that the reflection coefficient is sensitive to the change of D_1. With the increase of D_1, the resonance point shifts to low frequency; the impedance matching gradually deteriorates; and the -10 dB impedance bandwidth gradually narrows. When $D_1 = 7$ mm, S_{11} cannot be below -10 dB. When D_1 takes a larger value, the antenna's HPBW widens in the high frequency, but in the low frequency HPBW becomes narrower. In order to make the antenna have better impedance matching performance, $D_1 = 6$ mm is selected.

Figure 9 shows the variations of antenna reflection coefficient and HPBW with the length of the

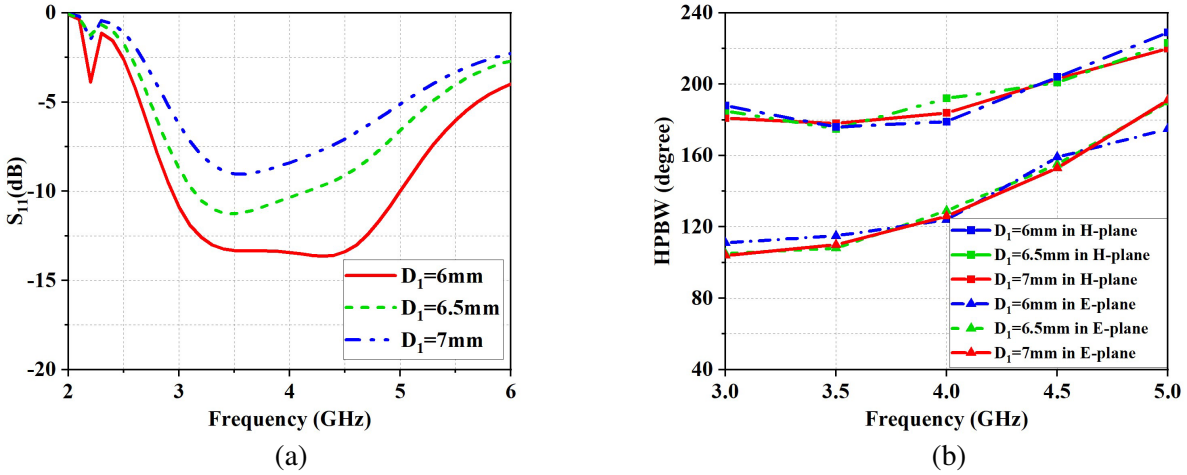

Figure 8. Simulated (a) S_{11} and (b) HPBW with different values of D_1.

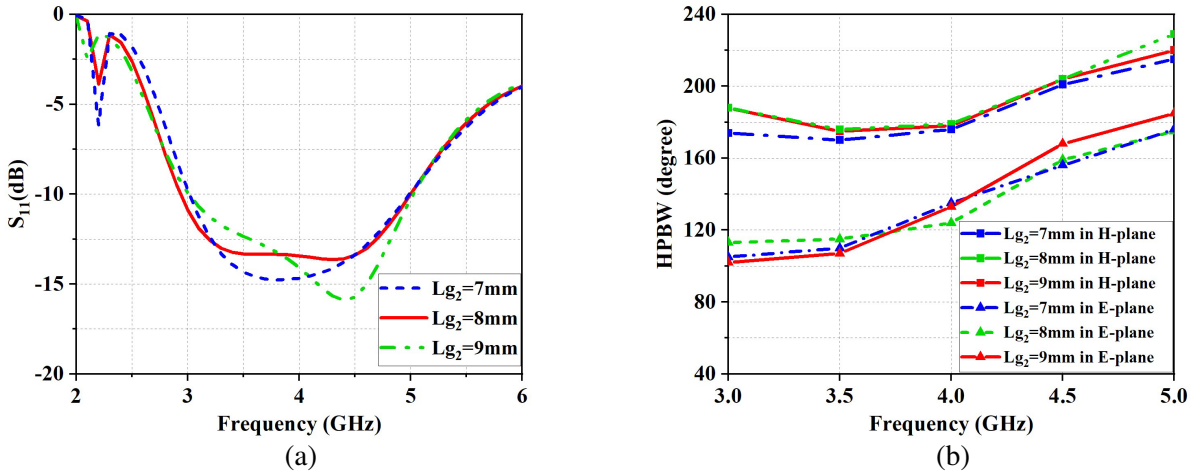

Figure 9. Simulated (a) S_{11} and (b) HPBW with different values of Lg_2.

inclined metal wall Lg_2. The change of Lg_2 has minor effect on the reflection coefficient. When the length of Lg_2 increases, the resonant point shifts slightly to the high frequency, but the -10 dB impedance bandwidth of the antenna is basically unchanged. When Lg_2 takes a larger value, the beamwidth of most frequencies is widened, but the beamwidth of E-plane at low frequency is narrow. Considering comprehensively, $Lg_2 = 8$ mm is selected.

Figure 10 shows the variation of antenna reflection coefficient and HPBW with feedline width Wf_1. The feedline width affects the input impedance of the antenna. When $Wf_1 = 1$ mm, the input impedance mismatches, and the reflection coefficient of the antenna does not reach below -10 dB. When $Wf_1 = 2$ mm and $Wf_1 = 3$ mm, a wide -10 dB impedance bandwidth can be achieved, but when $Wf_1 = 3$ mm, the frequency band shifts to high frequency. The feedline width has small influence on the beamwidth of different frequencies. To obtain the best bandwidth, $Wf_1 = 2$ mm is selected.

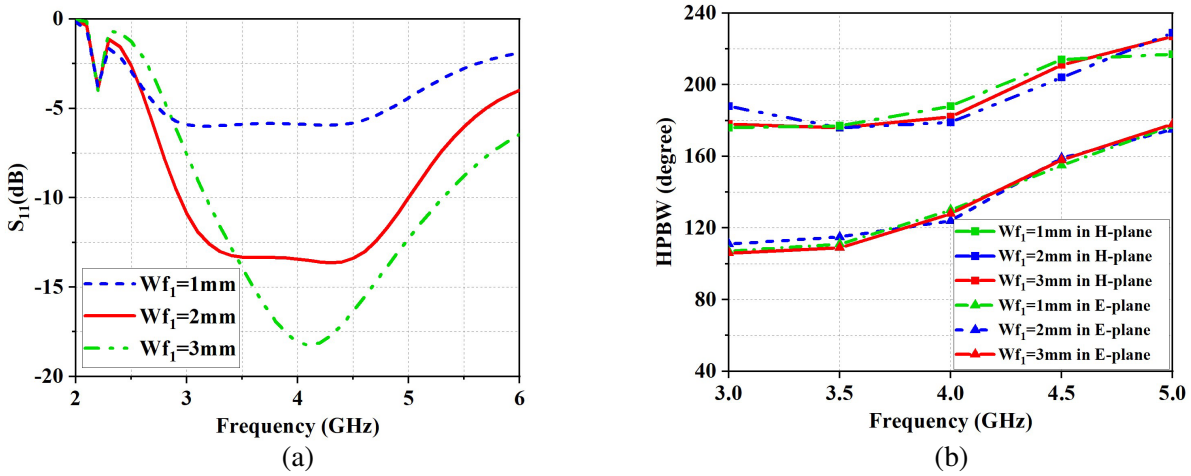

Figure 10. Simulated (a) S_{11} and (b) HPBW with different values of Wf_1.

3. EXPERIMENTAL RESULTS

The proposed antenna is fabricated and measured to verify the antenna performance. Considering the processing difficulty and cost, the ground of the antenna is made of aluminum, and the rest of the antenna is made of copper. Keysight E5063A vector network analyzer (VNA) is used to measure the

S_{11} of the antenna, and the far-field performance of the antenna is measured in a microwave anechoic chamber. Figure 11(a) shows a photograph of the fabricated antenna, and Figures 11(b)–11(c) show the measurement environment. The simulated and measured S_{11} curves of the antenna are shown in Figure 12(a). The simulation and measurement results of −10 dB IBW are 51.9% (2.94–5.0 GHz) and 56.8% (2.91–5.22 GHz), respectively. Compared with the simulation results, the measured IBW is wider, which is mainly caused by errors in antenna processing and welding. Figure 12(b) shows the simulated and measured gains. The antenna gain is stable at about 4 dBi in the operating bandwidth, and the simulated and measured gain curves are in good agreement.

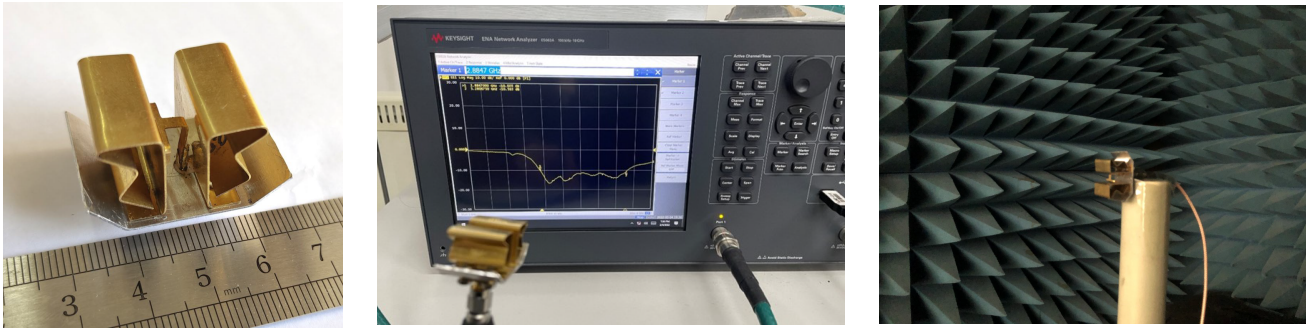

(a) (b) (c)

Figure 11. (a) Fabricated antenna, (b) measurement environment for antenna reflection coefficient, (c) measurement environment for antenna radiation performance.

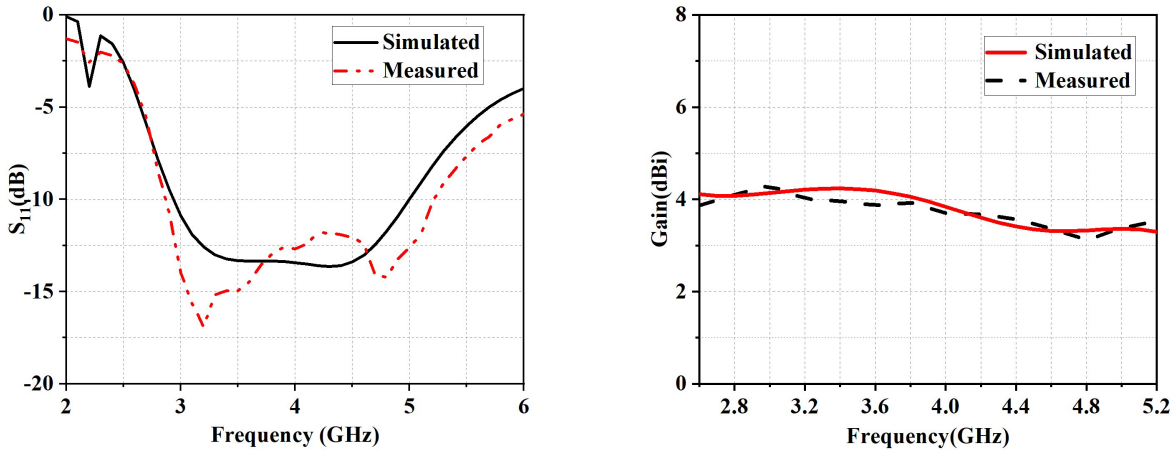

(a) (b)

Figure 12. (a) S_{11} and (b) gain of presented antenna.

Table 2. Simulation and measurement results of HPBW at different frequencies.

Frequency	*E*-plane		*H*-plane	
	Simulated	Measured	Simulated	Measured
3.2 GHz	112°	115°	185°	193°
3.7 GHz	117°	113°	179°	163°
4.2 GHz	137°	131°	188°	167°
4.7 GHz	165°	169°	217°	205°

Figure 13 shows the simulated and measured normalized radiation patterns at 3.2 GHz, 3.7 GHz, 4.2 GHz, and 4.7 GHz. It can be observed that the antenna has widebeam characteristics in the E and H planes at all these frequencies. Due to the features of magneto-electric dipole, the antenna has nearly symmetric patterns and low cross-polarization radiation at all frequencies. The small differences between the simulated and measured radiation patterns are attributed to the factors such as processing errors and minor noise in the measurement environment. The simulation and measurement results of HPBW at the four frequencies are listed in Table 2.

Table 3 shows the comparison between the presented and published wide-beam antennas, which indicates that the presented antenna has wider bandwidth and beamwidth, and more compact size.

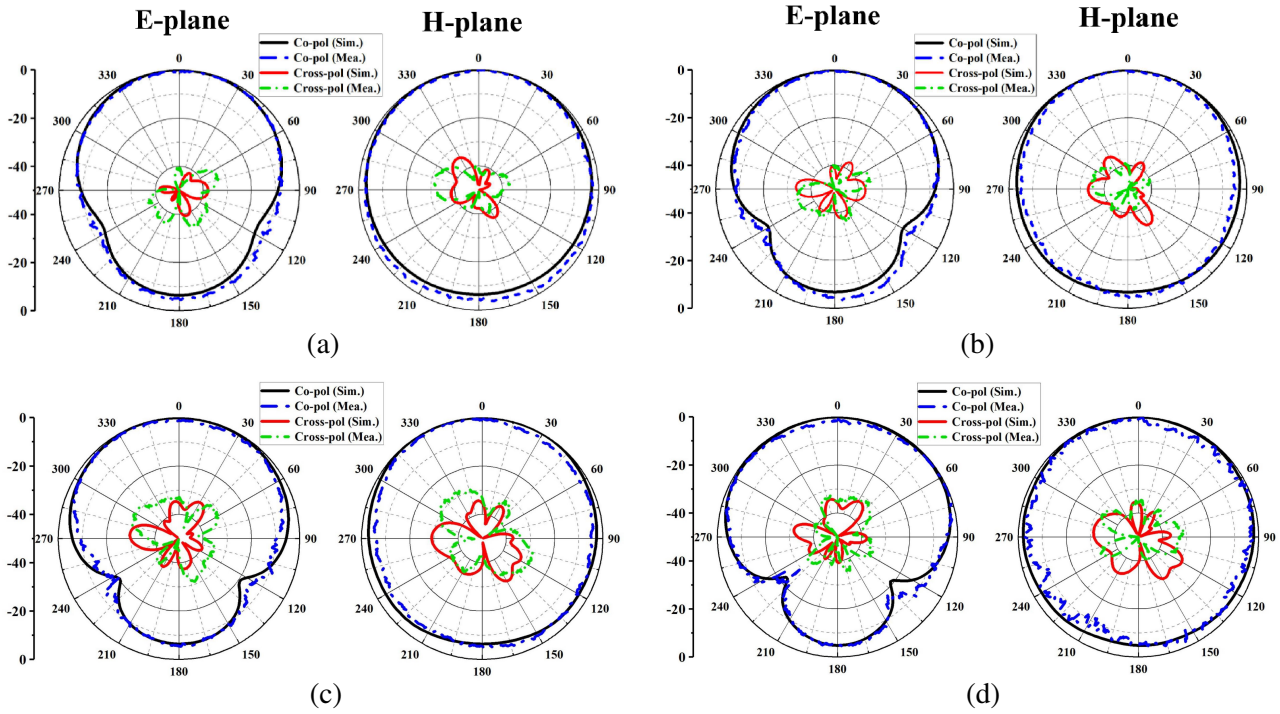

Figure 13. Radiation patterns at (a) 3.2 GHz, (b) 3.7 GHz, (c) 4.2 GHz and (d) 4.7 GHz.

Table 3. Performance comparison.

Ref.	Size (λ)	IBW	HPBW in E-plane	HPBW in H-plane	Peak Gain (dBi)
[6]	$1.03 * 1.03 * 0.43$	41% (1.9–2.7 GHz)	$78° < \theta < 80°$	$115° < \theta < 130°$	6.3
[7]	$0.72 * 0.62 * 0.2$	34.8% (1.9–2.7 GHz)	$94° < \theta < 104°$	$94° < \theta < 104°$	4.6
[10]	$0.73 * 0.57 * 0.36$	49% (7.8–13.2 GHz)	$107° < \theta < 125°$	$77° < \theta < 85°$	6.5
[15]	$0.68 * 0.56 * 0.2$	65.7% (2.05–3.95 GHz)	$75° < \theta$	$65° < \theta$	5
[16]	$0.83 * 0.83 * 0.31$	7.6% (3.02–3.26 GHz)	$171° < \theta < 210°$	$120° < \theta < 137°$	4
Prop.	$0.41 \times 0.27 \times 0.2$	56.8% (2.91–5.22 GHz)	$110° < \theta < 175°$	$163° < \theta < 229°$	4.4

4. CONCLUSION

In this paper, a wideband ME dipole antenna with wide-beam characteristics is presented. By loading bent metal plates on the electric dipoles, adding inclined metal walls on two sides of the ground, and modifying the structure of the feedline, the antenna realizes the characteristics of wideband and wide beam, and has stable gain in the operating bandwidth. The designed antenna also has compact size and low cross polarization radiation. It achieves a 56.8% -10 dB impedance bandwidth and realizes the HPBW of over 110° in E-plane and over 160° in H-plane throughout the operational bandwidth. The proposed antenna has potential application value in wideband wireless communication system.

REFERENCES

1. Wang, J., L. Zhou, and W. Chen, "A novel wide beam UWB antenna," *International Conference on Microwave and Millimeter Wave Technology*, 961–964, 2010.
2. Ko, S. and J. Lee, "Hybrid zeroth-order resonance patch antenna with broad E-plane beamwidth," *IEEE Transactions on Antennas and Propagation*, Vol. 61, No. 1, 19–25, 2012.
3. Wang, R., B.-Z. Wang, C. Hu, C. Gong, and X. Ding, "Low-profile on-board antenna with a broad beam based on three-current model," *Progress In Electromagnetics Research*, Vol. 156, 13–24, 2016.
4. Zhu, A., S. Wu, J. Shi, P. Hu, and J. Li, "Low profile wide beamwidth antenna fed by 1 : 5 unequal wilkinson power divider," *Progress In Electromagnetics Research Letters*, Vol. 99, 111–118, 2021.
5. Luk, K. M. and H. Wong, "A new wideband unidirectional antenna element," *International Journal of Microwave and Optical Technology*, Vol. 1, No. 1, 35–43, 2006.
6. Li, Y. and K. M. Luk, "A linearly polarized magnetoelectric dipole with wide H-plane beamwidth," *IEEE Transactions on Antennas and Propagation*, Vol. 62, No. 4, 1830–1836, 2014.
7. Qiu, W., C. Chen, and W. Chen, "A broadband magnetoelectric dipole antenna with stable wide beamwidth," *2016 IEEE International Symposium on Antennas and Propagation (APSURSI)*, 1849–1850, 2016.
8. Shuai, X., S. Xiao, X. Fan, and C. Gong, "A novel widebeam planar patch antenna for WLAN applications," *2016 11th International Symposium on Antennas, Propagation and EM Theory (ISAPE)*, 55–57, 2016.
9. Yang, G., S. Zhang, J. Li, Y. Zhang, and G. F. Pedersen, "A multi-band magneto-electric dipole antenna with wide beam-width," *IEEE Access*, Vol. 8, 68820–68827, 2020.
10. Yang, D., X.-L. Liang, R.-H. Jin, and J.-P. Geng, "A broadband printed slot antenna with wide E-plane beamwidth," *IEEE International Symposium on Antennas and Propagation (APSURSI)*, 1600–1601, 2014.
11. Yang, G., J. Li, D. Wei, and R. Xu, "Study on wide-angle scanning linear phased array antenna," *IEEE Transactions on Antennas and Propagation*, Vol. 66, No. 1, 450–455, 2018.
12. Wang, R., P. Gao, P. Wang, and K. Kang, "A planar end-fire antenna with wide beamwidth for 60 GHz applications," *Progress In Electromagnetics Research Letters*, Vol. 61, 125–130, 2016.
13. Duan, G. and F. Zhang, "Low profile SIW cavity-backed magneto-electric dipole with wide beamwidth radiation patterns," *2018 12th International Symposium on Antennas, Propagation and EM Theory (ISAPE)*, 1–3, 2018.
14. He, Y. and Y. Li, "Dual-polarized microstrip antennas with capacitive via fence for wide beamwidth and high isolation," *IEEE Transactions on Antennas and Propagation*, Vol. 68, No. 7, 5095–5103, 2020.
15. Idayachandran, G. and R. Nakkeeran, "Compact magneto-electric dipole antenna for LTE femtocell base stations," *Electronic Letters*, Vol. 52, No. 8, 574–576, 2016.
16. Sun, S., Y. Jiao, and Z. Weng, "Wide-beam dielectric resonator antenna with attached higher-permittivity dielectric slabs," *IEEE Antennas and Wireless Propagation Letters*, Vol. 19, No. 3, 462–466, 2020.